Host–Guest Systems | Hot Paper

International Edition: DOI: 10.1002/anie.201500635
German Edition: DOI: 10.1002/ange.201500635

Dynamic Inclusion Complexes of Metal Nanoparticles Inside Nanocups**

Mariana Alarcón-Correa, Tung-Chun Lee, and Peer Fischer**

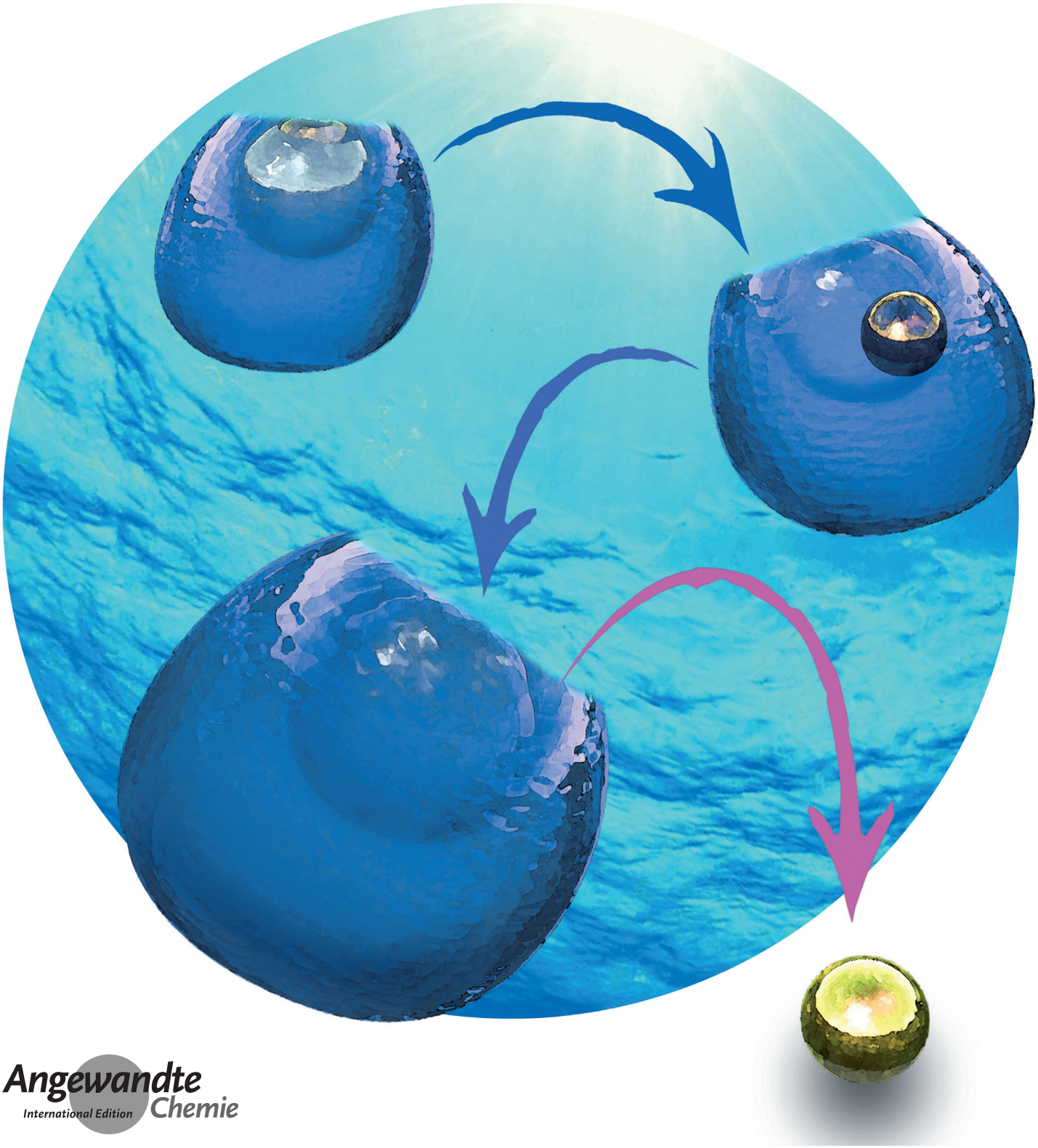

Abstract: *Host–guest inclusion complexes are abundant in molecular systems and of fundamental importance in living organisms. Realizing a colloidal analogue of a molecular dynamic inclusion complex is challenging because inorganic nanoparticles (NPs) with a well-defined cavity and portal are difficult to synthesize in high yield and with good structural fidelity. Herein, a generic strategy towards the fabrication of dynamic 1:1 inclusion complexes of metal nanoparticles inside oxide nanocups with high yield (>70%) and regiospecificity (>90%) by means of a reactive double Janus nanoparticle intermediate is reported. Experimental evidence confirms that the inclusion complexes are formed by a kinetically controlled mechanism involving a delicate interplay between bipolar galvanic corrosion and alloying–dealloying oxidation. Release of the NP guest from the nanocups can be efficiently triggered by an external stimulus.*

Encapsulation underpins a number of fundamental processes in living systems and occurs on multiple length scales, ranging from the inclusion of small molecules within enzymatic pockets to the compartmentalization in cells by lipid bilayers. Artificial encapsulation systems have been realized with macrocyclic molecules, liposomes, polymersomes, mesoporous materials,[1] and metal–organic frameworks (MOFs).[2] These systems show promise in catalysis and drug delivery.[3] However, the encapsulation of functional nanomaterials, for example, metal nanoparticles (NPs), within a well-defined nanoscale cavity remains challenging. Whereas NPs with a concave (negative) curvature, including nanobowls,[4] concave nanocubes,[5] and cap-shaped NPs,[6] have been reported, the formation of metal NP inclusion complexes has thus far not been demonstrated.

Herein, we report a generic scheme for the high-yield growth of oxide nanocups and their dynamic 1:1 inclusion complexes with metal NPs selectively located deep inside the cavity (Figure 1). The size of the nanocups lies between that of small viruses and large enzymes. The nanocups described herein encapsulate and can release an approximately 10 nm large gold NP (Au NP). The nanocups are readily functionalized, and their well-defined portal allows small molecules to access the cavity and the Au NP, which facilitates the triggered release of the NP. The nanocup could potentially be a means to stabilize the guest NPs in a number of environments, including solvents in which the NPs normally cannot be stably dispersed.

The generation of an inclusion complex of a Au NP inside a nanocup is achieved by a combination of physical vapor deposition (PVD) and wet chemical processes (Figure 1). First, block copolymer micelle nanolithography (BCML) is used to pattern a quasi-hexagonal array of monodisperse Au NPs (ca. 10 nm) on a large silicon wafer (Figure 1a).[7] In a second step, metallic silver is grown on the Au NPs by a Tollens reaction, yielding approximately 30 nm large Au–Ag Janus NPs (JNPs; see Figure 1b).[8] The thickness of the silver layer can be controlled by varying the reaction conditions. Then, an oxide material, such as SiO_2, TiO_2, or Al_2O_3, is deposited on the Ag layer by PVD glancing angle deposition (GLAD; Figure 1c).[9] The wafer is held at a shallow angle with respect to the vapor flux to permit shadow deposition only on the Au–Ag NPs (and not in the interstitial space). We have previously shown that the deposited materials smoothly interface with the seeds[10] and are evenly deposited on the NPs including the sides. The shape of the seed determines the morphology of the nanocup cavity (see below). The original seeds, which are Au–Ag JNPs themselves, now become Au–Ag–oxide double Janus NPs (d-JNPs), that is, JNPs of JNPs. These d-JNPs can then be efficiently removed from the wafer by sonication in aqueous ethanol (Figure 1d). A 1 cm^2 wafer sample contains approximately 2.0×10^{10} NPs, which can result in 1 mL of a nanocolloidal solution with a concentration comparable to that of commercially available Au nanocolloids of a similar size.[11] In the final fabrication step, the metallic silver is oxidized and dissolved upon the addition of hydrogen peroxide in the presence of aqueous ammonia. This results in 1:1 Au NP@nanocup inclusion complexes (Figure 1e).

Scanning electron microscopy (SEM) and transmission electron microscopy (TEM) were used to characterize the nanostructures. Statistical analysis of 500 NPs revealed that approximately 70% of the nanocups encapsulate one and only one Au NP. Multiple NP encapsulation was found to be negligible (<5%; see the Supporting Information, Section S4). The cavity dimensions are well controlled, with a standard deviation below 15%, demonstrating a high structural fidelity (Figure 2 and Section S5). Using angle-dependent TEM, we verified that the Au NP is indeed encapsulated deep inside the nanocup cavity (Figures S2 and S9).

Scanning TEM energy-dispersive X-ray (STEM-EDX) and energy-filtered TEM (EF-TEM) analyses were conducted on both the d-JNPs and the inclusion complexes to confirm the elemental compositions and distributions (Figures 3 and S4). Furthermore, to illustrate that our scheme is generic and permits the use of a range of functional materials, we have additionally fabricated 1:1 inclusion complexes of 1) Au NP@TiO_2 nanocups and 2) Au NP@Al_2O_3 nanocups (Figures S5 and S6).

[*] M. Alarcón-Correa, Dr. T.-C. Lee, Prof. Dr. P. Fischer
Max Planck Institute for Intelligent Systems
Heisenbergstrasse 3, 70569 Stuttgart (Germany)
E-mail: fischer@is.mpg.de
M. Alarcón-Correa, Prof. Dr. P. Fischer
Inst. for Phys. Chem., Univ. Stuttgart
Pfaffenwaldring 55, 70569 Stuttgart (Germany)
Dr. T.-C. Lee
Institute for Materials Discovery, University College London
Kathleen Lonsdale Building
Gower Place, London WC1E 6BT (UK)
E-mail: tungchun.lee@ucl.ac.uk

[**] We are grateful to C. Miksch and J. P. Spatz for help with SEM, BCML, and the Tollens reactions. We thank the Stuttgart Center for Electron Microscopy for TEM support. We are grateful to A. G. Mark for constructing the 3D models of the nanostructures and H.-H. Jeong for helpful comments. This work was in part supported by the European Research Council (ERC Grant 278213). The authors declare no competing financial interest.

Supporting information for this article is available on the WWW under http://dx.doi.org/10.1002/anie.201500635.

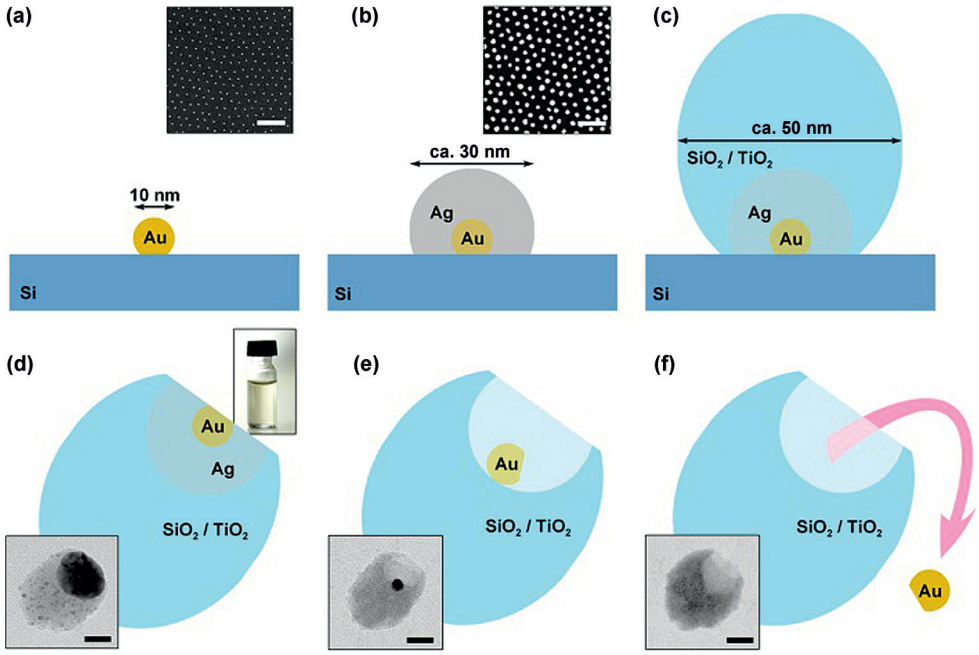

Figure 1. Fabrication scheme of 1:1 Au NP@nanocup inclusion complexes. a) Quasi-hexagonal pattern of Au NPs made by BCML. b) Au–Ag Janus NPs grown by a Tollens reaction. Insets (a and b): SEM images, scale bars: 200 nm. c) Oxide deposition by GLAD, to generate Au–Ag–oxide d-JNPs. d) Lift-off of d-JNPs by sonication. Top right inset: photo of the solution. e) A 1:1 inclusion complex is obtained upon oxidative dissolution of silver. f) Release of the Au NP guest triggered by an external stimulus, resulting in empty nanocups. Insets (e–f): TEM images, scale bars: 20 nm.

The Au NPs are almost all (over 90%) located deep inside the nanocup cavity (Section S6). While there is no material difference between the cavity and the outer surface of the nanocup, the curvature differs. However, this alone is not sufficient to explain the high tendency towards the formation of inclusion complexes in combination with the unexpectedly high specificity towards the binding ratio and location within the cavity in thermodynamic terms. Therefore, kinetic factors are very likely to play a crucial role. To gain a better understanding of the reaction intermediates, we monitored the silver distribution and the relative position of the Au NPs with EF-TEM in samples prepared from a quenched reaction mixture of the oxidation step (Figure 4). The proposed reaction scheme is as follows: Upon addition of H_2O_2 and $NH_{3(aq)}$ to the d-JNPs, reduction of H_2O_2 preferentially occurs on the cathodic region around the Au NPs (red arrow) while bipolar galvanic oxidation of metallic Ag is mediated by electron transfer across the Ag–Au interface (purple arrow), with silver(I) solubilized in the form of $[Ag(NH_3)_2]^+$ (green arrow; Figure 4 f). This is similar to the recently reported auto-polarization effects of the Cu–Pt bimetallic microswimmers.[12] In our case, the rate of oxidative dissolution is enhanced at the edge that is farthest away from the Au NP, leading to the formation of a pre-cavity (Figure 4 g). Nevertheless, when the solvent–silver interface retreats into the pre-cavity of the nanocup, diffusion of the solvated species around the interface—and hence the bipolar galvanic mechanism—is considerably hindered. At this stage, we suspect that diffusion processes become important, where Ag atoms diffuse through the Au NP via alloying or around the Au NP by surface diffusion and are directly oxidized on the gold surface

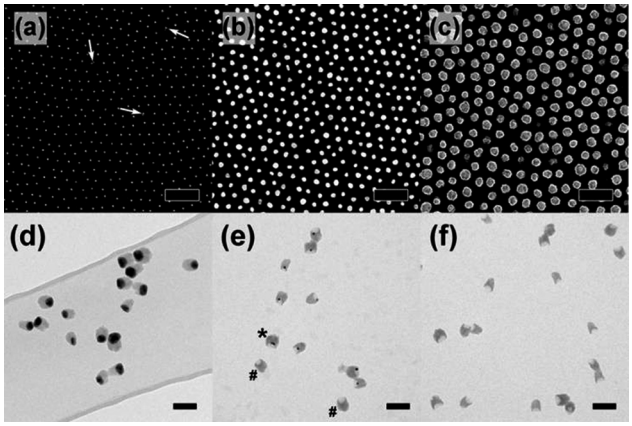

Figure 2. a–c) SEM images of an array of Au NPs (a; $d = 8 \pm 0.9$ nm, dimeric Au NPs are marked by white arrows), Au–Ag JNPs (b; $d = 32.8 \pm 4.5$ nm), and Au–Ag–SiO_2 d-JNPs (c, $d = 49.8 \pm 9.2$ nm). Scale bars: 200 nm. d–f) TEM images of Au–Ag–SiO_2 d-JNPs (d), Au NP@SiO_2 nanocup inclusion complexes (e; a 2:1 inclusion complex is marked by "*", and empty nanocups are marked by "#"), and empty SiO_2 nanocups obtained after decomplexation (f). Scale bars: 100 nm. The formation of 2:1 complexes is believed to be a result of dimeric Au NP seeds that originate from the BCML process. d = diameter.

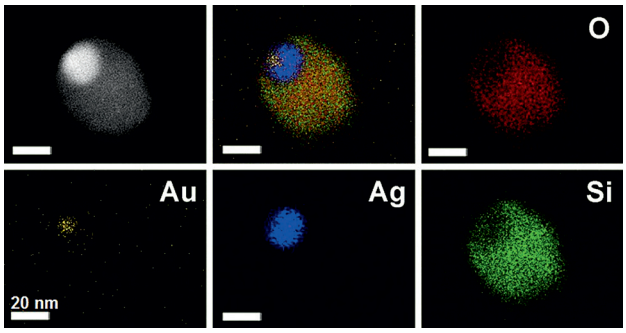

Figure 3. HAADF-STEM image and false-color STEM-EDX elemental maps of a Au–Ag–SiO_2 d-JNP. Scale bars: 20 nm. Color codes (and the corresponding transition edges): gold yellow (Au L), oxygen red (O K), silicon green (Si K), silver blue (Ag L).

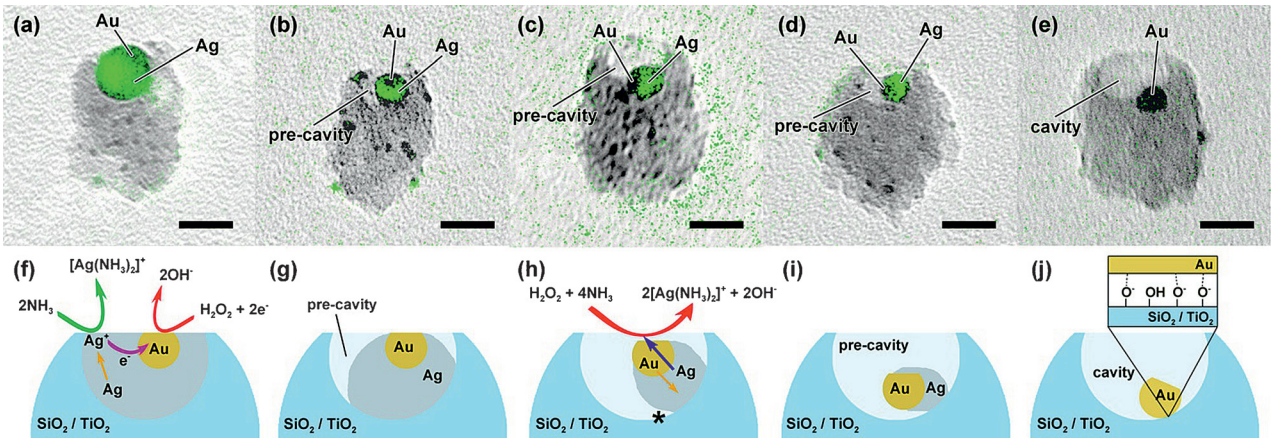

Figure 4. Proposed mechanism for the formation of the inclusion complexes. Silver distribution maps (green, Ag $M_{4,5}$) overlaid onto the corresponding bright-field TEM images of a Au–Ag–SiO_2 d-JNP (a), reaction intermediates (b–d), and a Au NP@SiO_2 nanocup inclusion complex (e). Scale bars: 20 nm. f–j) Respective schematic representations of the proposed formation mechanism.

(Figure 4h, red arrow). It has been reported that solid-phase diffusion processes are four to five orders of magnitude more pronounced for nanoparticles than in the bulk at room temperature.[13] The concentration gradient of silver atoms across the Au NP is maintained by the continuous oxidative dissolution of silver on the outer surface of the Au NP. This outward atomic flux of silver results in a net displacement of the Au NP in the opposite direction towards the bottom of the nanocup cavity. As diffusion of silver in gold is faster than that of gold in silver,[14] vacancies and voids within the silver will be created (Kirkendall effect), which would then enhance the rate of dissolution of silver by the bipolar galvanic mechanism (positive feedback). After a combination of galvanic and alloying–dealloying corrosion, the Au NP eventually docks at the bottom of the newly formed nanocup cavity and binds with the negatively charged oxide groups formed in an alkaline environment (Figure 4j). This alloying–dealloying mechanism explains why >90% of the Au NPs are found deep inside the cavity. We note that a bipolar galvanic reaction alone would lead to an "immature" release of the Au NP and hence a much lower yield of inclusion complexes plus a random distribution of Au NPs within the cavity.

Our system differs from yolk–shell nanoparticles[15] in the way that regiospecific binding and triggered release of the guest NP can only be achieved in our case. As the Au NP is stabilized in the nanocup by the negatively charged oxide groups on the SiO_2 surface, the encapsulated Au NP can be efficiently released upon a decrease in pH value (causing protonation of the surface oxide groups) or addition of a competitive ligand, such as a water-soluble thiol, resulting in a solution of free Au NPs and empty oxide nanocups (Figure 1f and 2f, see also Figures S3, S10, and S11).

In summary, we have realized a nanocolloidal analogue of a supramolecular host–guest system consisting of oxide nanocup hosts and their metal-nanoparticle guests. A parallel bottom-up growth scheme was used to first fabricate double Janus nanoparticles, which are reacted in solution to yield the metal NP@nanocups complexes. A kinetically controlled bipolar galvanic corrosion and an alloying–dealloying effect result in nanocups of high yield and very high structural fidelity with a single Au NP at a well-defined location inside. We have also demonstrated the triggered release of the NP guest in response to an external stimulus. To the best of our knowledge, this is the first dynamic metal NP inclusion complex. It opens possibilities in stabilizing NPs in solvent environments where the NPs would otherwise not form stable colloidal solutions. This can be achieved without directly functionalizing the metal NPs. Furthermore, the confined geometrical inclusion of the metal NP may open possibilities in the targeted delivery of molecules or reactive NPs. The confined geometry can be used to realize a catalytic nanoreactor with a defined structure.

Experimental Section

Materials: Polystyrene (1056)-block-poly(2-vinylpyridine) (495) was supplied by Polymer Source, Canada. Silicon (100) wafers were supplied by CrysTec GmbH, Germany. All chemicals are analytical grade and were used as received unless otherwise stated. Deionized water with 18.2 MΩ resistivity was generated by a Milli-Q ultrapure system.

The preparation of the Au NP array, the growth of metallic Ag on the Au NP seeds, and the deposition of ceramic materials were conducted based on modified procedures of previous reports and are detailed in the Supporting Information. The d-JNPs were lifted off from the wafer by sonicating a sample wafer piece (ca. 1 cm^2) in 50% (v/v) aqueous ethanol for ca. 20 min, resulting in a pure nanocolloidal solution. To 1 mL of this solution, aqueous ammonia (10 μL, 4.0 M) and H_2O_2 (20 μL, 0.8% w/w) were added. After 15 min, the 1:1 inclusion complexes were separated by centrifugation (12100 g, 60 min). The supernatant was removed, and the inclusion complexes were re-dispersed in 1 mL of 50% aqueous ethanol by sonication. To release the Au NPs from the nanocups, 25 μL of concentrated HNO_3 (15 M) was added to the solution of inclusion complexes. After 30 min, the empty nanocups were separated by centrifugation (12100 g, 60 min). The supernatant was removed, and the empty nanocups were re-dispersed in 50% aqueous ethanol by sonication.

Keywords: host–guest systems · inclusion complexes · Janus nanoparticles · nanocups · nanostructures

How to cite: *Angew. Chem. Int. Ed.* **2015**, *54*, 6730–6734
Angew. Chem. **2015**, *127*, 6834–6838

[1] M. Liong, S. Angelos, E. Choi, K. Patel, J. F. Stoddart, J. I. Zink, *J. Mater. Chem.* **2009**, *19*, 6251–6257.
[2] M. Kiguchi, J. Inatomi, Y. Takahashi, R. Tanaka, T. Osuga, T. Murase, M. Fujita, T. Tada, S. Watanabe, *Angew. Chem. Int. Ed.* **2013**, *52*, 6202–6205; *Angew. Chem.* **2013**, *125*, 6322–6325.
[3] a) F. Hof, S. L. Craig, C. Nuckolls, J. Rebek, Jr., *Angew. Chem. Int. Ed.* **2002**, *41*, 1488–1508; *Angew. Chem.* **2002**, *114*, 1556–1578; b) X. J. Loh, J. del Barrio, P. P. C. Toh, T.-C. Lee, D. Jiao, U. Rauwald, E. A. Appel, O. A. Scherman, *Biomacromolecules* **2012**, *13*, 84–91; c) D. Jiao, J. Geng, X. J. Loh, D. Das, T.-C. Lee, O. A. Scherman, *Angew. Chem. Int. Ed.* **2012**, *51*, 9633–9637; *Angew. Chem.* **2012**, *124*, 9771–9775.
[4] Y. Ridelman, G. Singh, R. Popovitz-Biro, S. G. Wolf, S. Das, R. Klajn, *Small* **2012**, *8*, 654–660.
[5] a) J. A. Zhang, M. R. Langille, M. L. Personick, K. Zhang, S. Y. Li, C. A. Mirkin, *J. Am. Chem. Soc.* **2010**, *132*, 14012–14014; b) T. Yu, D. Y. Kim, H. Zhang, Y. Xia, *Angew. Chem. Int. Ed.* **2011**, *50*, 2773–2777; *Angew. Chem.* **2011**, *123*, 2825–2829.
[6] a) Y. M. Lee, M. A. Garcia, N. A. F. Huls, S. H. Sun, *Angew. Chem. Int. Ed.* **2010**, *49*, 1271–1274; *Angew. Chem.* **2010**, *122*, 1293–1296; b) N. N. Zhao, L. S. Li, T. Huang, L. M. Qi, *Nanoscale* **2010**, *2*, 2418–2423.
[7] R. Glass, M. Möller, J. P. Spatz, *Nanotechnology* **2003**, *14*, 1153–1160.
[8] S. Kruss, V. Srot, P. A. van Aken, J. P. Spatz, *Langmuir* **2012**, *28*, 1562–1568.
[9] M. M. Hawkeye, M. J. Brett, *J. Vac. Sci. Technol. A* **2007**, *25*, 1317–1335.
[10] A. G. Mark, J. G. Gibbs, T.-C. Lee, P. Fischer, *Nat. Mater.* **2013**, *12*, 802–807.
[11] http://www.sigmaaldrich.com/catalog/product/aldrich/742015?lang=de&region=DE.
[12] R. Liu, A. Sen, *J. Am. Chem. Soc.* **2011**, *133*, 20064–20067.
[13] E. González, J. Arbiol, V. F. Puentes, *Science* **2011**, *334*, 1377–1380.
[14] Y. Sun, Y. Xia, *J. Am. Chem. Soc.* **2004**, *126*, 3892–3901.
[15] J. Liu, S. Z. Qiao, J. S. Chen, X. W. (D.) Lou, X. Xing, G. Q. (M.) Lu, *Chem. Commun.* **2011**, *47*, 12578–12591.

Received: February 11, 2015
Published online: May 8, 2015

